Published in final edited form as:
Hepatology. 2012 December ; 56(6): 2316–2327. doi:10.1002/hep.25938.

Nicotinamide Adenine Dinucleotide Phosphate Oxidase (NOX) in Experimental Liver Fibrosis: GKT137831 as a Novel Potential Therapeutic Agent

Tomonori Aoyama[1),2)], **Yong-Han Paik**[3)], **Sumio Watanabe**[2)], **Benoît Laleu**[4)], **Francesca Gaggini**[4)], **Laetitia Fioraso-Cartier**[4)], **Sophie Molango**[4)], **Freddy Heitz**[4)], **Cédric Merlot**[4)], **Cédric Szyndralewiez**[4)], **Patrick Page**[4)], and **David A. Brenner**[1)]

Tomonori Aoyama: aoyama@juntendo.ac.jp; Yong-Han Paik: yhpaik@yuhs.ac; Sumio Watanabe: sumio@juntendo.ac.jp; Benoît Laleu: benoit.laleu@genkyotex.com; Francesca Gaggini: francesca.gaggini@genkyotex.com; Laetitia Fioraso-Cartier: lfc@genkyotex.com; Sophie Molango: sophie.molango@genkyotex.com; Freddy Heitz: freddy.heitz@genkyotex.com; Cédric Merlot: dric.merlot@genkyotex.com; Cédric Szyndralewiez: dric.szyndralewiez@genkyotex.com; Patrick Page: patrick.page@genkyotex.com; David A. Brenner: dbrenner@ucsd.edu

[1)]Department of Medicine, University of California San Diego, La Jolla, CA [2)]Department of Gastroenterology, Juntendo University School of Medicine, Tokyo, Japan [3)]Department of Internal Medicine, Samsung Medical Center, Sungkyunkwan University School of Medicine [4)]GenKyoTex SA, 16 Chemin des Aulx, 1228 Plan-Les-Ouates, Geneva, Switzerland

Abstract

Background & Aims—NADPH oxidase (NOX) generates reactive oxygen species (ROS) in hepatic stellate cells (HSCs) during liver fibrosis. In response to fibrogenic agonists, such as angiotensin II (Ang II), the NOX1 components form an active complex including Rac1. Superoxide dismutase 1 (SOD1) interacts with the NOX-Rac1 complex to stimulate NOX activity. NOX4 is also induced in activated HSCs/myofibroblast by increased gene expression. Here, we investigate the role of an enhanced activity SOD1 G37R mutation (SODmu) and the effects of GKT137831, a dual NOX1/4 inhibitor, on HSCs and liver fibrosis.

Methods—To induce liver fibrosis, wild-type (WT) and SOD1mu mice were treated with carbon tetrachloride (CCl_4) or bile duct ligation (BDL). Then, to address the role of NOX-SOD1-mediated ROS production in HSC activation and liver fibrosis, mice were treated with a NOX1/4 inhibitor. Fibrosis and ROS generation was assessed by histology and measurement of TBARS and NOX related genes. Primary cultured HSCs isolated from WT, SODmu, and NOX1 knock-out (KO) mice were assessed for ROS production, Rac1 activity, and NOX gene expression.

Correspondence: David A. Brenner, Department of Medicine, 1318A Biomedical Sciences Building, 9500 Gilman Drive, University of California San Diego, La Jolla, CA 92093-0602, Phone: 858-534-1501; Fax: 858-822-0084; dbrenner@ucsd.edu.

Author Contributions: Tomonori Aoyama: acquisition, analysis and interpretation of all data except Fig. 2, drafting of the manuscript, and statistical analysis. Yong-Han Paik: interpretation of data, and technical support. Sumio Watanabe: study supervision. Sophie Molango: acquisition of screening data, analysis and interpretation of data. Laetitia Fioraso-Cartier: development of screening assays and acquisition of data. Freddy Heitz: screening assays design, interpretation of data, and technical support, critical revision of manuscript. Cédric Szyndralewiez: in vivo pharmacokinetic data generation and collection, in vivo vehicle development. Cédric Merlot: computer-aided drug design of small molecule. Benoît Laleu: Synthesis and design of small molecules, screening data analysis. Francesca Gaggini: Synthesis and design of small molecule, screening data analysis. Patrick Page, design of small molecule, ADME and PK data analysis and interpretation, molecule selection, critical revision of manuscript, drug discovery and development supervision. David A. Brenner: study concept and design, analysis and interpretation of data, critical revision of manuscript for important intellectual content, and study supervision.

Disclosures: Benoît Laleu, Francesca Gaggini, Laetitia Fioraso-Cartier, Sophie Molango, Freddy Heitz, Cédric Merlot, Cédric Szyndralewiez, Patrick Page are employees of GenKyoTex SA, which developed and provided the drug GKT137831used in this study.

Results—Liver fibrosis was increased in SOD1mu mice, and ROS production and Rac1 activity were increased in SOD1mu HSCs. The NOX1/4 inhibitor GKT137831 attenuated liver fibrosis and ROS production in both SOD1mu and WT mice as well as mRNA expression of fibrotic and NOX genes. Treatment with GKT137831 suppressed ROS production and NOX and fibrotic gene expression, but not Rac1 activity, in SOD1mut and WT HSCs. Both Ang II and TGFb upregulated NOX4, but AngII required NOX1.

Conclusions—SOD1mu induces excessive NOX1 activation through Rac1 in HSCs, causing enhanced NOX4 upregulation, ROS generation, and liver fibrosis. Treatment targeting NOX1/4 may be a new therapy for liver fibrosis.

Keywords

NADPH oxidase; SOD1; reactive oxidative species; hepatic stellate cells

Introduction

Most chronic liver diseases produce liver fibrosis, which results from the loss of hepatocytes combined with the accumulation of extracellular matrix (ECM) proteins, mainly collagen(1). Hepatic stellate cells (HSCs) play a key role in the response to hepatotoxic injury and are a major source of ECM proteins(2). Liver injury activates quiescent HSCs to become myofibroblasts. Numerous studies have now demonstrated that advanced liver fibrosis in patients and in experimental rodent models is reversible(3–5). However, the only effective therapy to treat hepatic fibrosis to date is to remove the causative agent, so there is an unmet clinical need to develop new specific therapies for liver fibrosis.

Oxidative stress results from an inappropriate balance between the production and clearance of reactive oxidative species (ROS) and leads to aberrant tissue repair in the liver. NADPH oxidase (NOX) is an enzyme system that catalyzes the reduction of molecular oxygen to superoxide. NOX in HSCs induces specific intracellular signaling that results in activation(6). The NOX family consists of seven different members (NOX1-5 and the dual oxidases Duox1 and -2)(7). Among the NOX family, both NOX1, NOX2 (also named $gp91^{phox}$), and NOX4 are expressed on HSCs and may contribute to liver fibrosis(6, 8). Bone marrow (BM) chimeric mice demonstrated that liver fibrosis requires NOX2 generated ROS from both BM derived inflammatory cells and endogenous liver cells, including HSCs, while NOX1 is required from only endogenous liver cells[6]. Furthermore, NOX1 knockout (NOX1KO) HSCs have less ROS generation than NOX2 knockout (NOX2KO) HSCs(6). Therefore, we suggest that NOX1 is more crucial than NOX2 in the generation of ROS in HSCs. Upon stimulation with agonists such as angiotensin II (Ang II), the cytosolic subunits, including Rac-GTP, translocate to the membrane-bound cytochrome complex, to produce enzymatically active NOX1 and NOX2(9). On the other hand, NOX4 activity is regulated by increased expression of its protein, including during myofibroblast/HSC activation(10–12). In particular, TGF-β signaling increases the protein expression and activity of NOX through the increase in NOX4 gene transcription, not via agonist induced complex formation(7).

Superoxide dismutase 1 (SOD1) interacts with Rac1 in the active NOX complex to stimulate NOX activity(13). Mutations in SOD1, such as G93A and G37R, that are associated with familial amyotrophic lateral sclerosis (ALS)(14), increase NOX activity to produce increased ROS in glial cells in the brain(13) and in other organs, including the liver(15). However, the interaction between wild-type (WT) or mutant SOD1 with NOX in HSCs and in liver fibrosis is unknown.

Because of this evidence incriminating NOX1 and NOX4 in the pathogenesis of liver fibrosis, we aimed to assess the effectiveness of treatment with GKT137831, a NOX1/4 inhibitor, on the development of liver fibrosis. We furthermore wanted to investigate the role of SOD1 in NOX activity and liver fibrosis. We hypothesized that mice with the SOD1 G37R mutation (SOD1mu) with increased catalytic activity would have increased ROS generation and increased liver fibrosis.

Materials and Methods

Chemical GKT137831

2-(2-chlorophenyl)-4-[3-(dimethylamino)phenyl]-5-methyl-1H- pyrazolo[4,3-c]pyridine-3,6(2H,5H)-dione was provided by Genkyotex S.A, Plan-Les-Ouates (Geneva), Switzerland(16). GKT137831 is a drug-like small molecule that was identified through High-throughput Screening, followed by medicinal chemistry efforts involving hit-to-lead and lead optimisation campaigns(17).

Animal models of liver fibrosis

Specific pathogen-free, wild-type (WT) C57BL/6J mice were purchased from the Jackson Laboratory. SOD1 G37R mutant mice in a C57BL/6 background were a gift from Dr. Don Cleveland of the University of California, San Diego(18). NOX1 knockout (NOX1KO) mice in a C57BL/6 background were developed by KH Krause as described (19). For the carbon tetrachloride (CCl_4) model of liver fibrosis, 6 week old male mice were injected intraperitoneally with CCl_4, which was diluted 1:3 in corn oil (Sigma), or with vehicle (corn oil) at a dose of 0.5 μL/g of body weight twice a week for a total of 12 injections. During the last half of CCl_4 treatment, mice were treated with 60 mg/kg of the NOX1/4 inhibitor GKT137831 (GenKyoTex, Geneva, Switzerland) or vehicle by intragastric injection daily. Mice were sacrificed 48 hours after the last CCl_4 injection. For the bile duct ligation (BDL) model, 6 week old male mice were anesthetized. After laparotomy, the common bile duct was ligated twice and the abdomen closed. The sham operation was performed similarly without BDL. From 11 days after operation, mice were treated with 60 mg/kg of the NOX1/4 inhibitor GKT137831 or vehicle by daily intragastric lavage. Mice were sacrificed 21 days after operation. Serum levels of alanine aminotransferase (ALT) were measured with a commercial kit (Thermo Scientific). The mice received humane care according to the National Institutes of Health recommendations outlined in Guide for the care and Use of Laboratory Animals. All animal experiments were approved by the institutional animal care and use committees and performed at the University of California San Diego.

Histological Analysis

For immunohistochemical analysis, liver specimens were fixed in 10% buffered formalin and were incubated with monoclonal antibody against α-SMA (Sigma) with an M.O.M. kit (Vector Laboratories), or rat anti-mouse F4/80 (eBioscience). For immunofluorescent staining, frozen sections were incubated with antibody to SOD1 (Binding Site), desmin (Neomarkers), or 4-hydroxynoneal (Alpha Diagnostic), and this was followed by imaging with fluorescent microscopy(20).

Western blotting and Immunoprecipitation

The preparation of whole cell protein extracts from frozen livers, electrophoresis, and subsequent blotting were performed as previously described(21). Blots were with mouse antibody to α-SMA and β-actin (Sigma) and then visualized them with the enhanced chemiluminescence light method (Thermo Scientific). Immunoprecipitation of Rac1 was performed in a LX-2 human HSC cell line. 15 cm dishes of LX-2 cells were pretreated with

Ang II or PBS for 30 minutes. Proteins were extracted and incubated with mouse anti-Rac1 agarose conjugate antibody (Millipore) for 4°C overnight with rotating. Beads were washed 5 times with lysis buffer. Pellets were resuspended in SDS-PAGE sample buffer and incubated at 95° for 5 minutes. Western blotting was performed as described using primary antibodies to SOD1 (Binding site) and Rac1 (Santa Cruz).

Isolation of Liver Cells Fractions

Liver cells of WT mice were fractionated into four major cell populations (hepatocytes, macrophages, endothelial cells and HSCs) with documentation of purity as described(6).

Quantitative Real-Time Polymerase Chain Reaction (PCR)

Total RNA was prepared from cells or frozen livers, reverse-transcribed, and quantitated by real-time PCR, as described(20). PCR primer sequences are listed in the Supplemental information. The expression of respective genes was normalized to 18S RNA as an internal control.

Thiobarbituric Acid Reactive Substances Determination

Hepatic lipid peroxidation was assessed by measuring thiobarbituric acid reactive substances (TBARS) formation(6). Details are given in the Supplemental Information.

HSC Isolation, Cell Culture and Treatment

Mouse HSCs were isolated using a two-step collagenase-pronase perfusion of mouse livers followed by 8.2% Nycodenz (Accurate Chemical and Scientific Corp) two-layer discontinuous density gradient centrifugation as described(20). After isolation, HSCs were seeded on uncoated plastic tissue culture dishes and cultured in Dulbecco's modified Eagle's medium (DMEM) (GIBCO BRL; Life Technologies Inc.) supplemented with 10% fetal bovine serum (FBS). HSCs isolated from WT, SOD1 mutant or NOX1KO mice were cultured in DMEM with 10% FBS. After 48 hours of incubation, the medium was changed into 1% FBS, and cells were then incubated with 10^{-6} M Ang II (Sigma) or vehicle [phosphate-buffered saline (PBS)] with 20 μM NOX1/4 inhibitor or vehicle (PBS) for 24 hours.

Measurement of Collagen-Driven GFP expression in HSCs

To measure collagen promoter activity, HSCs (1×10^5 cell/well) were isolated from WT or SOD1 mutant collagen promoter-driven GFP transgenic (colI-GFP) mice (pCol9GFP-HS4,5 transgene)(22). SOD1 mutant coll-GFP mice were made by crossing WT coll-GFP mice with SOD1 mutant mice. HSCs were incubated with 10^{-6} M Ang II (Sigma) or vehicle (PBS) with 20 μM NOX1/4 inhibitor or vehicle (PBS)) for 24 hours. The number of GFP-positive cells was determined via the counting of GFP-positive cells in 10 randomly chosen high-power fields.

Measurement of ROS Generation in HSCs

HSCs were preincubated with the redox-sensitive dye DCFDA (10 μM)(Molecular Probes) for 20 minutes and then stimulated with 10^{-6} M Ang II (Sigma) or vehicle (PBS) with 20 μM NOX1/4 inhibitor or vehicle (PBS). DCFDA fluorescence was measured with a multiwall fluorescence scanner (Fluostar Optima; BMG Labtech)(6).

Rac1 activity assay

Rac1 activity in HSCs was determined with the Rac1 G-LISA™ activation assay kit. (Cytoskelton, Inc.). Briefly, WT or SOD1 mutant HSCs were treated by 10^{-6} M Ang II

(Sigma) or vehicle (PBS) with 20 μM NOX1/4 inhibitor or vehicle (PBS) for 24 hours. According to the manufacturer's protocol, protein lysate was extracted and Rac1 activity was determined by luminescence intensity.

Statistical Analysis

Data were expressed as means ± standard error of the mean (SEM). Statistical differences between means were determined using Student t tests or analysis of variance (ANOVA) on ranks followed by a post hoc test (Student-Newman-Keuls all pairwise comparison procedures) as appropriate. P values less than 0.05 were considered statistically significant.

Results

SOD1 expression is increased in HSCs in CCl_4 induced fibrotic liver

SOD1 mRNA levels were increased in the livers of WT mice after CCl_4-induced liver fibrosis (Fig. 1A). To investigate the cellular source of SOD1 in fibrotic liver, we measured mRNA expression of SOD1 in hepatocytes, macrophages/Kupffer cells, and HSCs isolated from vehicle- or CCl_4 treated mice. SOD1 expression was significantly increased in HSCs after CCl_4 treatment, but not in hepatocytes or in macrophages (Fig. 1B). As detected by fluorescence microscopy, the number of SOD1 and desmin positive HSCs was markedly increased in CCl_4 treated liver compared to vehicle control (Fig. 1C, D). These results indicate that the upregulation of SOD1 in HSCs is related to the development of liver fibrosis.

GKT137831 is a novel, specific dual NOX1/4 inhibitor

In an effort to discover new selective modulators of Nox enzymes, we developed cell free assays using membranes prepared from cells heterologously over-expressing a specific Nox enzyme isoform (23, 24). GKT137831 (Fig. 2A) is a potent Nox4 inhibitor (Ki =120 ± 30 nM) with an affinity similar to the irreversible and unspecific flavoprotein inhibitor Diphenyliodonium (DPI; Ki =70±10 nM) (Fig. 2B). As expected, DPI showed complete non-selectivity, and the same potency was recorded on all four Noxes probed (Fig. 2B). On the other hand, GKT137831 had a better potency both on human Nox4 (Ki =140 ± 40 nM) and human Nox1 (Ki =110± 30 nM) and was found 15-fold less potent on Nox2 (Ki = 1750 ± 700 nM) and 3-fold less potent on Nox5 (Ki =410±100 nM). Moreover, GKT137831 did not significantly inhibit a highly-specific NOX2-driven response, i.e. neutrophil oxidative burst up to 100uM, as measured by flow cytometry in human whole blood. Also, the compound did not show any immunosuppressive activity through potential inhibition of Nox2 when administered at 100mg/kg orally in an *in vivo* murine model of staphylococcus aureus killing (data not shown). We demonstrated GKT137831 to be specific for NADPH oxidases over other flavoprotein-containing oxidases and also excluded the possibility that GKT137831 is a general ROS scavenger: GKT137831 was further tested in a xanthine oxidase assay using similar ROS production methodology as in our proprietary NOX assays and with the same read-out. Whereas DPI showed high affinity (Ki=50nM) consistent with its non-specific mechanism of action, GKT137831 demonstrated no affinity for xanthine oxidase (Ki>100μM) (Fig. 2B and 2C) as well as the inability to scavenge superoxide ($O_2^{\bullet-}$), the common end product of Nox proteins and xanthine oxidase. To further demonstrate the specificity of GKT137831 for Nox enzymes, our candidate drug was subjected to an extensive *in vitro* off-target pharmacological profile on 170 different proteins including ROS producing and redox-sensitive enzymes, as well as representative proteins of well recognized drug target families such as GPCRs, kinases, ion channels and others enzymes(25). GKT137831 when tested at 10 μM did not show any significant inhibition of any tested target protein, demonstrating the excellent specificity of this compound (see supplementary Table 2).

GKT137831 prevents liver fibrosis in WT and SOD1mu mice

To investigate the role of SOD1 and the effect of NOX1/4 inhibition on liver fibrosis, liver fibrosis was induced in SOD1mu (with increased catalytic activity) and WT mice by 12 consecutive CCl_4 injections over a 6-week period. During the last half of CCl_4 injections, some mice were treated with GKT137831 daily. CCl_4-induced liver fibrosis was more pronounced in SOD1mu compared to WT mice. Liver fibrosis in both SOD1mu and WT mice was attenuated by GKT137831 treatment. The NOX1/4 inhibitor reduced the levels of hepatic collagen deposition in CCl_4 induced fibrosis in SOD1mu and WT mice to the same low level, as assessed by Sirius red staining and its quantification (Fig. 3A,B). Hepatic α-SMA expression, a marker for HSC activation, was enhanced in SOD1mu mice after CCl_4 injections compared to WT mice, as assessed by immunohistochemistry and immunoblotting. The increased hepatic α-SMA expression was markedly decreased in SOD1mu mice treated with GKT137831, to a level similar to that of WT mice given the NOX1/4 inhibitor (Fig. 3C,D). The mRNAs of fibrogenic markers, including collagen α1(I), tissue inhibitor of metalloprotease 1 (TIMP-1), and TGF-β were increased in SOD1mu mice to higher levels than in WT mice after CCl_4 injections, but treatment with GKT137831 reduced the induction of those genes to the same lower levels (Fig. 3E). Similarly, BDL-induced hepatic fibrosis in both WT and SOD1mu mice was decreased by treatment with GK137831 (Supplemental Figure 1). Thus, both hepatotoxin (CCl4) (this study) and cholestasis (BDL) (this study and REFA) induced liver fibrosis is suppressed by blocking NOX1 and NOX4.

GKT137831 blocks hepatic inflammation in WT and SOD1mu mice

To investigate the role of SOD1 and the effect of NOX1/4 inhibition on liver inflammation, macrophage infiltration and activation were evaluated. After CCl_4 treatment, the expression of F4/80 and CD68, a macrophage activation marker, was significantly increased in SOD1mu livers versus WT livers, as determined by immunohistochemistry and quantitative real-time PCR. However, NOX1/4 inhibition prevented macrophage infiltration and activation to levels similar to those observed in mice untreated with CCl_4 (Fig. 4A-C). Hepatic mRNA expression of TNF-α was also increased in SOD1mu mice after CCl_4 treatment, but this increase was suppressed by GKT137831 (Fig. 4D). Serum ALT levels were increased in CCl_4 treated SOD1mu mice compared to CCl_4 treated WT mice, which was also reduced by NOX1/4 inhibition by GKT137831 (Fig. 4E). These results indicate that increased liver inflammation and injury in CCl_4 treated SOD1mu and WT mice was inhibited to similar lower levels by GKT137831 treatment.

Nox 1/4 inhibition decreases hepatic lipid peroxidation in WT and SOD1mu mice

To investigate ROS mediated lipid peroxidation, we measured the lipid peroxidation products 4-hydroxynonenal (4-HNE) and malondialdehyde (MDA), as indicators of oxidative stress in the liver. Hepatic 4-HNE levels were increased in SOD1mu mice compared to WT mice after CCl_4 treatment, but this increase was suppressed by inhibition of NOX1/4 (Fig. 5A). Measurement of MDA using TBARS showed that increased hepatic MDA levels in SOD1mu mice were suppressed by GKT137831 treatment after CCl_4 injections (Fig. 5B). In agreement with liver fibrosis and inflammation results, the levels of hepatic lipid peroxidation in CCl_4 treated SOD1mu mice were decreased to the same low level as WT mice by Nox 1/4 inhibition.

GKT137831 inhibits the expression of fibrogenic and NOX genes in HSCs

We used activation of primary cultures of HSCs as a model of activated myofibroblasts(26, 27). Primary HSCs were isolated from both WT and SOD1mu mice. In quiescent HSCs, mRNA expression of collagen α1(I) and Acta2 are at the same low level. The mRNA levels

in activated SOD1mu HSCs were significantly greater than in activated WT HSCs (Fig. 5C). Incubating with GKT137831 reduced the expression levels of collagen α1(I) and Acta2 mRNA to the same low levels in both activated SOD1mu and WT HSCs (Fig. 5C). Interestingly, mRNA expression of NOX4 and to a lesser extent NOX1 was increased in activated SOD1mu HSCs compared to WT HSCs, and this increase was also suppressed by GKT137831 (Fig. 5D).

GKT137831 blocks the fibrogenic response and ROS production induced by Ang II in WT and SOD1mu HSCs

Next, we assessed HSC activation by measuring GFP fluorescence in quiescent HSCs purified from the ColI-GFP reporter mouse, in which the collagen α1(I) promoter/enhancer drives GFP. Ang II induced higher GFP fluorescence in SOD1mu HSCs than in WT HSCs, but this GFP enhancement was suppressed by GKT137831 (Fig. 6A, B). To assess the effect of SOD1mu on ROS generation, we measured the quantity of ROS in DCFDA-loaded HSCs after Ang II treatment. Ang II induced excessive ROS production in SOD1mu HSCs compared to WT HSCs. GKT137831 suppressed ROS generation in SOD1mu HSCs to the same levels as WT HSCs treated with the NOX1/4 inhibitor (Fig. 6C).

To investigate whether SOD1 interacts with Rac1 in response to Ang II, we performed co-immunoprecipitation experiments for SOD1 and Rac1 in cell extracts from the human HSC LX-2 cell line. SOD1 was pulled down strongly by Rac1 after Ang II stimulation in HSCs (Fig. 6D). Because the NOX-Rac complex stimulates NOX activity, we assessed Rac1 activity in HSCs after Ang II treatment. Rac1 activity increased more in SOD1mu HSCs stimulated with Ang II than in WT HSCs. As expected, treatment with GKT137831 had no effect on Rac1 activity after Ang II stimulation (Fig. 6E). Taken together, these results indicate that the SOD1mut activates HSCs by forming a complex with and activating Rac1. Treatment with GKT137831 inhibits ROS generation, but does not regulate Rac1 activity in both WT and SOD1mu HSCs.

SOD1 G37R mutation enhances NOX4 upregulation through NOX1 in HSCs

To further investigate the relationship between NOX1, NOX4, and SOD1, HSCs were isolated from WT, SOD1mu, and NOX1KO mice. In response to Ang II, induction of NOX4 mRNA expression was suppressed in NOX1KO HSCs compared to WT HSCs (Fig. 7A). These results indicate that NOX1 is required for NOX4 upregulation in HSCs stimulated with Ang II. Ang II increased mRNA expression of both NOX1 and NOX4 in SOD1mut HSCs to a greater extent than in WT HSCs. Treatment with GKT137831 suppressed these increases to the same low levels in both SOD1mut and WT HSCs (Fig. 7A). Similarly, Ang II increased the mRNA expression of collagen α1(I) and TIMP-1 more in SOD1mu HSCs compared to WT HSCs. The induction of these fibrogenic genes was blocked in the NOX1 KO HSCs as well as by treatment of WT and SOD1mu HSCs with the NOX1/4 inhibitor (Fig. 7B). On the other hand, TGF-β induces NOX4 in HSCs independent of NOX1 (Fig. 7C).

Discussion

Expression of NOX isoforms is increased in patients with pulmonary(28), renal (29), and liver fibrosis(30). Furthermore, NOX isoforms are induced and are required for experimental murine models of pulmonary(10), renal(31), and liver fibrosis(32). HSCs require NOX for the fibrogenic effects of angiotensin II(32), leptin(33), PDGF(34), TGF-β(10), advanced glycation end products(35), and phagocytosis(36). Thus, NOX is a core mediator(37) that is essential to convert an initial stimulus to the development(37) of experimental and clinical fibrosis in multiple organs. Our current study extends our understanding of the role of NOX

in hepatotoxic and cholestatic liver fibrosis by demonstrating that: (1) The catalytically active SOD1mut G37R increases liver fibrosis in mice. (2) GKT137831, a novel, first-in-class, NOX 1/4 inhibitor, blocks liver fibrosis in SOD1mu and WT mice. (3) SOD1, Rac1 and Nox1 interact to induce ROS and activate HSCs. (3) AngII induces Nox4 expression via Nox1 in HSCs. (4) SOD1mu HSCs have increased fibrotic gene expression, increased ROS production and increased Rac1 activity. (5) GKT137831 blocks the activation of SOD1mu and WT HSCs. Thus, SOD1, NOX1, and NOX4 interact in the HSC to generate ROS and induce liver fibrosis.

SOD1, Rac1 and Nox1 interact to induce ROS to activate HSCs and produce liver fibrosis

In normal cellular homeostasis, SOD1 converts superoxide to hydrogen peroxide to eliminate ROS(38). Indeed, treatment with an adenovirus vector encoding the SOD1 gene improved ethanol induced liver injury through reducing free radical adducts in rats(39). However, SOD1 also interacts with NOX, and certain SOD1 mutations(40) induce the activation of NOX, thereby causing additional ROS production in tissues(13, 15, 41). ROS derived from NOX have an important role in the development of liver fibrosis(6, 32, 42). In the current study, we demonstrate that SOD1 G37R mutation worsens CCl_4 induced liver fibrosis by increasing NOX1/4 expression, Rac1 activity, and ROS generation in HSCs (Fig. 3–6). The mechanism for our observation is provided by the recent studies showing that SOD1 stabilized Rac1 which is one of the cytosolic subunits interacting with NOX. Specific SOD1 mutations induce higher activation of NOX by maintaining Rac1 in its active GTP-bound form thereby causing excessive ROS production and injuring cells(13, 43). Consistent with these reports, our results demonstrate that SOD1 interacts with Rac1, and SOD1mut enhances Rac1 activity in HSCs treated with Ang II (Fig. 6D, E). Thus, we propose that the SOD1/Rac1/NOX interaction is a core mediator in HSC activation and fibrosis, including the fibrogenic actions of Angiotensin II on HSCs. Indeed, mRNA expression of NOX1 and NOX4 was increased, accompanied by enhanced fibrogenic responses in activated SOD1mu HSCs compared to activated WT HSCs (Fig. 5C,D). Harraz et al focused on NOX2 as a target of SOD1-Rac1 component in glial cells(13). Since NOX2 and NOX1 share components including Rac1 for their activation(7), and we showed that NOX1 is more important for ROS generation in HSCs than NOX2(6), targeting NOX1 is crucial for inhibiting excessive ROS production in HSCs under fibrotic liver.

AngII induces Nox4 expression via Nox1 in HSCs

NOX4 is regulated at the level of gene transcription, not by the post-translational assembly of components into a complex(7). NOX4 is located downstream of TGF-β signaling and is an important molecule in the activation of myofibroblasts(10–12). Activation of the TGF-β-Nox4 pathway has been shown to have strong pro-fibrotic activity in cardiac fibrosis[12], kidney fibrosis[13] and lung fibrosis[11,19]. Inhibition of Nox4 in activated myofibroblast either by knock-down with siRNA, or with the non specific irreversible NOX antagonist DPI, prevented fibrosis in both pulmonary[11] and kidney[13] fibrosis. In our study, NOX4 mRNA levels were increased in activated and Ang II stimulated SOD1mu HSCs to a higher level than in WT HSCs (Fig. 5D, 7A). These results suggest that SOD1 regulates NOX4 induction. However, there are no studies reporting a direct interaction between SOD1 and NOX4. Our study provides insight into this relationship. First, because Ang II-induced NOX4 mRNA expression was inhibited in NOX1KO HSCs compared to WT HSCs (Fig. 7A), NOX1 induces NOX4 upregulation in HSCs. Thus, excessive activation of NOX1 by SOD1mut can lead to increased NOX4 expression in HSCs (Fig. 5D, 7A). Second, previous reports demonstrated that Rac1 may regulate NOX4 in several cells(44–46). Thus, increased Rac1 activity in SOD1mu HSCs may induce NOX4 upregulation (Fig. 6E, 7C). Third, increased phosphorylation of Smad2/3, which is downstream of TGF-β signaling, was

observed in the spinal cords of SOD1 mutant mice(47), demonstrating that an activating SOD1 mutation leads to activation of TGF-β signaling (Fig. 7C).

GKT137831, a novel, first-in-class, NOX 1/4 inhibitor blocks liver fibrosis in SOD1mu and WT mice

The present study demonstrates the interaction between SOD1, NOX1, and NOX4 to generate ROS in HSCs and induce liver fibrosis. Building on the work of us(6, 30, 32, 34, 42) and others(8, 35, 36, 48), this study establishes a role for Nox1 and Nox4 in generating oxidative damage to induce liver fibrosis. Treatment with GKT137831, a novel, first-in-class, specific Nox1/Nox4 inhibitor(17), reverses the fibrogenic response by inhibiting ROS production and expression of fibrogenic genes in both WT and SOD1mut HSCs. Most importantly, GKT137831 blocks liver fibrosis and downregulates the markers of oxidative stress, inflammation, and fibrosis in WT and SOD1mut mice. Taken together, these results indicate that dual inhibition of Nox1 and Nox4 might provide a unique opportunity for the treatment of liver fibrosis and other fibrotic diseases.

Supplementary Material

Refer to Web version on PubMed Central for supplementary material.

Acknowledgments

Grant Support: 1 R24 DK090962, 5 P50 AA011999, 5 R01 GM041804, American Liver Foundation

Abbreviations

Ang II	angiotensin II
α-SMA	alpha-smooth muscle actin
ALT	alanine aminotransferase
CCl_4	carbon tetrachloride
CM-H_2DCFDA	2′7′-dichlorofluorescein diacetate
ECM	extracellular matrix
GFP	green fluorescent protein
FBS	fetal bovine serum
HSC	hepatic stellate cell
KO	knockout
NADPH	nicotinamide adenine dinucleotide phosphate
NOX	NADPH oxidase
PBS	phosphate buffered saline
PCR	polymerase chain reaction
ROS	reactive oxidative species
SOD	superoxide dismutase
TBARS	thiobarbituric acid reactive substances
TGF	transforming growth factor

TIMP	tissue inhibitor of metalloproteinase
TNF	tumor necrosis factor
WT	wild-type

References

1. Bataller R, Brenner DA. Liver fibrosis. J Clin Invest. 2005; 115:209–218. [PubMed: 15690074]
2. Friedman SL. Mechanisms of hepatic fibrogenesis. Gastroenterology. 2008; 134:1655–1669. [PubMed: 18471545]
3. Fink SA, Jacobson IM. Managing patients with hepatitisB-related or hepatitisC-related decompensated cirrhosis. Nat Rev Gastroenterol Hepatol. 2011; 8:285–295. [PubMed: 21695841]
4. Klein S, Mittendorfer B, Eagon JC, Patterson B, Grant L, Feirt N, Seki E, et al. Gastric bypass surgery improves metabolic and hepatic abnormalities associated with nonalcoholic fatty liver disease. Gastroenterology. 2006; 130:1564–1572. [PubMed: 16697719]
5. Popov Y, Schuppan D. Targeting liver fibrosis: strategies for development and validation of antifibrotic therapies. Hepatology. 2009; 50:1294–1306. [PubMed: 19711424]
6. Paik YH, Iwaisako K, Seki E, Inokuchi S, Schnabl B, Osterreicher CH, Kisseleva T, et al. The nicotinamide adenine dinucleotide phosphate oxidase (NOX) homologues NOX1 and NOX2/gp91(phox) mediate hepatic fibrosis in mice. Hepatology. 2011; 53:1730–1741. [PubMed: 21384410]
7. Barnes JL, Gorin Y. Myofibroblast differentiation during fibrosis: role of NAD(P)H oxidases. Kidney Int. 2011; 79:944–956. [PubMed: 21307839]
8. Cui W, Matsuno K, Iwata K, Ibi M, Matsumoto M, Zhang J, Zhu K, et al. NOX1/nicotinamide adenine dinucleotide phosphate, reduced form (NADPH) oxidase promotes proliferation of stellate cells and aggravates liver fibrosis induced by bile duct ligation. Hepatology. 2011; 54:949–958. [PubMed: 21618578]
9. Brown DI, Griendling KK. Nox proteins in signal transduction. Free Radic Biol Med. 2009; 47:1239–1253. [PubMed: 19628035]
10. Hecker L, Vittal R, Jones T, Jagirdar R, Luckhardt TR, Horowitz JC, Pennathur S, et al. NADPH oxidase-4 mediates myofibroblast activation and fibrogenic responses to lung injury. Nat Med. 2009; 15:1077–1081. [PubMed: 19701206]
11. Cucoranu I, Clempus R, Dikalova A, Phelan PJ, Ariyan S, Dikalov S, Sorescu D. NAD(P)H oxidase 4 mediates transforming growth factor-beta1-induced differentiation of cardiac fibroblasts into myofibroblasts. Circ Res. 2005; 97:900–907. [PubMed: 16179589]
12. Bondi CD, Manickam N, Lee DY, Block K, Gorin Y, Abboud HE, Barnes JL. NAD(P)H oxidase mediates TGF-beta1-induced activation of kidney myofibroblasts. J Am Soc Nephrol. 2010; 21:93–102. [PubMed: 19926889]
13. Harraz MM, Marden JJ, Zhou W, Zhang Y, Williams A, Sharov VS, Nelson K, et al. SOD1 mutations disrupt redox-sensitive Rac regulation of NADPH oxidase in a familial ALS model. J Clin Invest. 2008; 118:659–670. [PubMed: 18219391]
14. Cleveland DW. From Charcot to SOD1: mechanisms of selective motor neuron death in ALS. Neuron. 1999; 24:515–520. [PubMed: 10595505]
15. Miana-Mena FJ, Gonzalez-Mingot C, Larrode P, Munoz MJ, Olivan S, Fuentes-Broto L, Martinez-Ballarin E, et al. Monitoring systemic oxidative stress in an animal model of amyotrophic lateral sclerosis. J Neurol. 2011; 258:762–769. [PubMed: 21108037]
16. Page, P.; Orchard, M.; Laleu, B.; Gaggini, F., inventors. Pyrazolo pyridine dione derivatives as NADPH oxidase inhibitors. Switzerland patent WO 2010/035221. 2010.
17. Laleu B, Gaggini F, Orchard M, Fioraso-Cartier L, Cagnon L, Houngninou-Molango S, Gradia A, et al. First in class, potent, and orally bioavailable NADPH oxidase isoform 4 (Nox4) inhibitors for the treatment of idiopathic pulmonary fibrosis. J Med Chem. 2010; 53:7715–7730. [PubMed: 20942471]

18. Wong PC, Pardo CA, Borchelt DR, Lee MK, Copeland NG, Jenkins NA, Sisodia SS, et al. An adverse property of a familial ALS-linked SOD1 mutation causes motor neuron disease characterized by vacuolar degeneration of mitochondria. Neuron. 1995; 14:1105–1116. [PubMed: 7605627]
19. Gavazzi G, Banfi B, Deffert C, Fiette L, Schappi M, Herrmann F, Krause KH. Decreased blood pressure in NOX1-deficient mice. FEBS Lett. 2006; 580:497–504. [PubMed: 16386251]
20. Aoyama T, Inokuchi S, Brenner DA, Seki E. CX3CL1-CX3CR1 interaction prevents carbon tetrachloride-induced liver inflammation and fibrosis in mice. Hepatology. 2010; 52:1390–1400. [PubMed: 20683935]
21. Aoyama T, Ikejima K, Kon K, Okumura K, Arai K, Watanabe S. Pioglitazone promotes survival and prevents hepatic regeneration failure after partial hepatectomy in obese and diabetic KK-A(y) mice. Hepatology. 2009; 49:1636–1644. [PubMed: 19205029]
22. Magness ST, Bataller R, Yang L, Brenner DA. A dual reporter gene transgenic mouse demonstrates heterogeneity in hepatic fibrogenic cell populations. Hepatology. 2004; 40:1151–1159. [PubMed: 15389867]
23. Palicz A, Foubert TR, Jesaitis AJ, Marodi L, McPhail LC. Phosphatidic acid and diacylglycerol directly activate NADPH oxidase by interacting with enzyme components. J Biol Chem. 2001; 276:3090–3097. [PubMed: 11060300]
24. Serrander L, Cartier L, Bedard K, Banfi B, Lardy B, Plastre O, Sienkiewicz A, et al. NOX4 activity is determined by mRNA levels and reveals a unique pattern of ROS generation. Biochem J. 2007; 406:105–114. [PubMed: 17501721]
25. Data of in vitro off-target pharmacological profile were generated by two independent and well established contract research organizations, accordingly to their protocols and in vitro assays developed: Cerep (<http://www.cerep.fr/>) and Millipore (<http://www.millipore.com/>).
26. Friedman SL, Arthur MJ. Activation of cultured rat hepatic lipocytes by Kupffer cell conditioned medium. Direct enhancement of matrix synthesis and stimulation of cell proliferation via induction of platelet-derived growth factor receptors. J Clin Invest. 1989; 84:1780–1785. [PubMed: 2556445]
27. De Minicis S, Seki E, Uchinami H, Kluwe J, Zhang Y, Brenner DA, Schwabe RF. Gene expression profiles during hepatic stellate cell activation in culture and in vivo. Gastroenterology. 2007; 132:1937–1946. [PubMed: 17484886]
28. Amara N, Goven D, Prost F, Muloway R, Crestani B, Boczkowski J. NOX4/NADPH oxidase expression is increased in pulmonary fibroblasts from patients with idiopathic pulmonary fibrosis and mediates TGFbeta1-induced fibroblast differentiation into myofibroblasts. Thorax. 2010; 65:733–738. [PubMed: 20685750]
29. Djamali A, Vidyasagar A, Adulla M, Hullett D, Reese S. Nox-2 is a modulator of fibrogenesis in kidney allografts. Am J Transplant. 2009; 9:74–82. [PubMed: 18976289]
30. Colmenero J, Bataller R, Sancho-Bru P, Dominguez M, Moreno M, Forns X, Bruguera M, et al. Effects of losartan on hepatic expression of nonphagocytic NADPH oxidase and fibrogenic genes in patients with chronic hepatitis C. Am J Physiol Gastrointest Liver Physiol. 2009; 297:G726–734. [PubMed: 19628656]
31. Sedeek M, Callera G, Montezano A, Gutsol A, Heitz F, Szyndralewiez C, Page P, et al. Critical role of Nox4-based NADPH oxidase in glucose-induced oxidative stress in the kidney: implications in type 2 diabetic nephropathy. Am J Physiol Renal Physiol. 2010; 299:F1348–1358. [PubMed: 20630933]
32. Bataller R, Schwabe RF, Choi YH, Yang L, Paik YH, Lindquist J, Qian T, et al. NADPH oxidase signal transduces angiotensin II in hepatic stellate cells and is critical in hepatic fibrosis. J Clin Invest. 2003; 112:1383–1394. [PubMed: 14597764]
33. De Minicis S, Seki E, Oesterreicher C, Schnabl B, Schwabe RF, Brenner DA. Reduced nicotinamide adenine dinucleotide phosphate oxidase mediates fibrotic and inflammatory effects of leptin on hepatic stellate cells. Hepatology. 2008; 48:2016–2026. [PubMed: 19025999]
34. Adachi T, Togashi H, Suzuki A, Kasai S, Ito J, Sugahara K, Kawata S. NAD(P)H oxidase plays a crucial role in PDGF-induced proliferation of hepatic stellate cells. Hepatology. 2005; 41:1272–1281. [PubMed: 15915457]

35. Guimaraes EL, Empsen C, Geerts A, van Grunsven LA. Advanced glycation end products induce production of reactive oxygen species via the activation of NADPH oxidase in murine hepatic stellate cells. J Hepatol. 2010; 52:389–397. [PubMed: 20133001]
36. Zhan SS, Jiang JX, Wu J, Halsted C, Friedman SL, Zern MA, Torok NJ. Phagocytosis of apoptotic bodies by hepatic stellate cells induces NADPH oxidase and is associated with liver fibrosis in vivo. Hepatology. 2006; 43:435–443. [PubMed: 16496318]
37. Mehal WZ, Iredale J, Friedman SL. Scraping fibrosis: expressway to the core of fibrosis. Nat Med. 2011; 17:552–553. [PubMed: 21546973]
38. De Minicis S, Brenner DA. NOX in liver fibrosis. Arch Biochem Biophys. 2007; 462:266–272. [PubMed: 17531188]
39. Lehmann TG, Wheeler MD, Schwabe RF, Connor HD, Schoonhoven R, Bunzendahl H, Brenner DA, et al. Gene delivery of Cu/Zn-superoxide dismutase improves graft function after transplantation of fatty livers in the rat. Hepatology. 2000; 32:1255–1264. [PubMed: 11093732]
40. Rosen DR. Mutations in Cu/Zn superoxide dismutase gene are associated with familial amyotrophic lateral sclerosis. Nature. 1993; 364:362. [PubMed: 8332197]
41. Marchetto MC, Muotri AR, Mu Y, Smith AM, Cezar GG, Gage FH. Non-cell-autonomous effect of human SOD1 G37R astrocytes on motor neurons derived from human embryonic stem cells. Cell Stem Cell. 2008; 3:649–657. [PubMed: 19041781]
42. De Minicis S, Seki E, Paik YH, Osterreicher CH, Kodama Y, Kluwe J, Torozzi L, et al. Role and cellular source of nicotinamide adenine dinucleotide phosphate oxidase in hepatic fibrosis. Hepatology. 2010; 52:1420–1430. [PubMed: 20690191]
43. Boillee S, Cleveland DW. Revisiting oxidative damage in ALS: microglia, Nox, and mutant SOD1. J Clin Invest. 2008; 118:474–478. [PubMed: 18219386]
44. Gorin Y, Ricono JM, Kim NH, Bhandari B, Choudhury GG, Abboud HE. Nox4 mediates angiotensin II-induced activation of Akt/protein kinase B in mesangial cells. Am J Physiol Renal Physiol. 2003; 285:F219–229. [PubMed: 12842860]
45. Chai D, Wang B, Shen L, Pu J, Zhang XK, He B. RXR agonists inhibit high-glucose-induced oxidative stress by repressing PKC activity in human endothelial cells. Free Radic Biol Med. 2008; 44:1334–1347. [PubMed: 18206668]
46. Wu RF, Ma Z, Myers DP, Terada LS. HIV-1 Tat activates dual Nox pathways leading to independent activation of ERK and JNK MAP kinases. J Biol Chem. 2007; 282:37412–37419. [PubMed: 17940286]
47. Nakamura M, Ito H, Wate R, Nakano S, Hirano A, Kusaka H. Phosphorylated Smad2/3 immunoreactivity in sporadic and familial amyotrophic lateral sclerosis and its mouse model. Acta Neuropathol. 2008; 115:327–334. [PubMed: 18210139]
48. Jiang JX, Chen X, Serizawa N, Szyndralewicz C, Page P, Schroder K, Brandes RP, et al. Liver fibrosis and hepatocyte apoptosis are attenuated by GKT137831, a novel NOX4/NOX1 inhibitor in vivo. Free Radic Biol Med. 2012

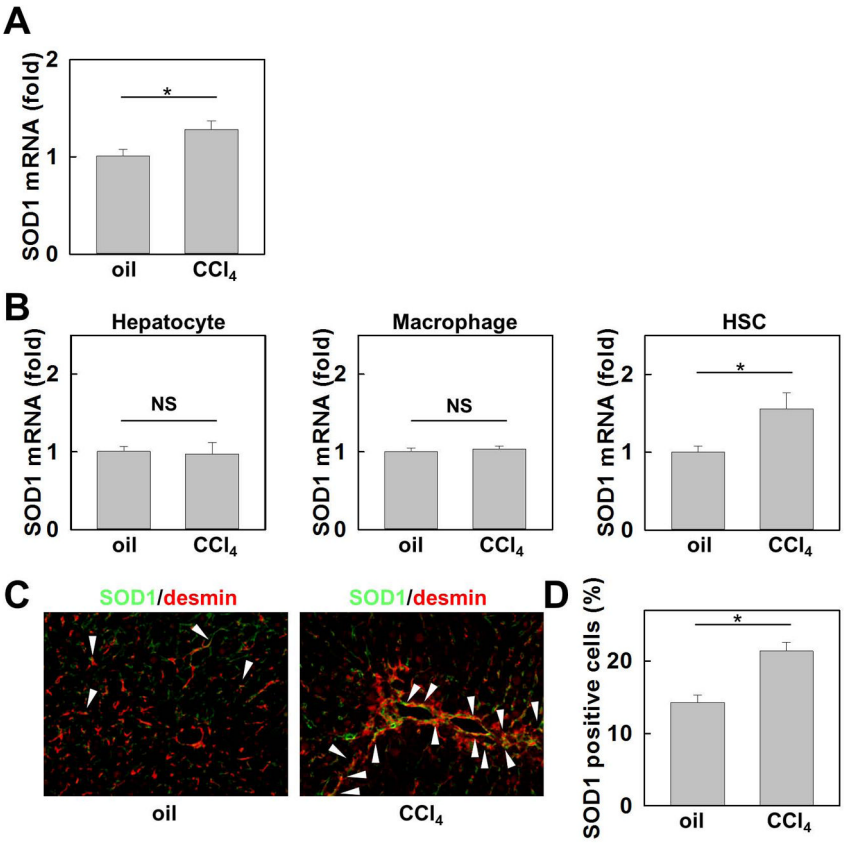

Fig. 1. SOD1 expression is enhanced in hepatic stellate cells (HSCs) in the fibrotic liver

Livers from WT mice were analyzed after 12 injections of CCl_4 or vehicle (n=5) (A) Hepatic mRNA expression of SOD1 was measured by quantitative real-time PCR. (B) mRNA levels of SOD1 in hepatocytes, macrophages, and HSCs isolated from vehicle- or CCl_4 treated WT mice detected by quantitative real-time PCR (n=3). (C) SOD1 expression (green) was detected by fluorescence microscopy via containing with desmin (red). (D) Percentage of SOD1 positive cells in desmin positive cells.

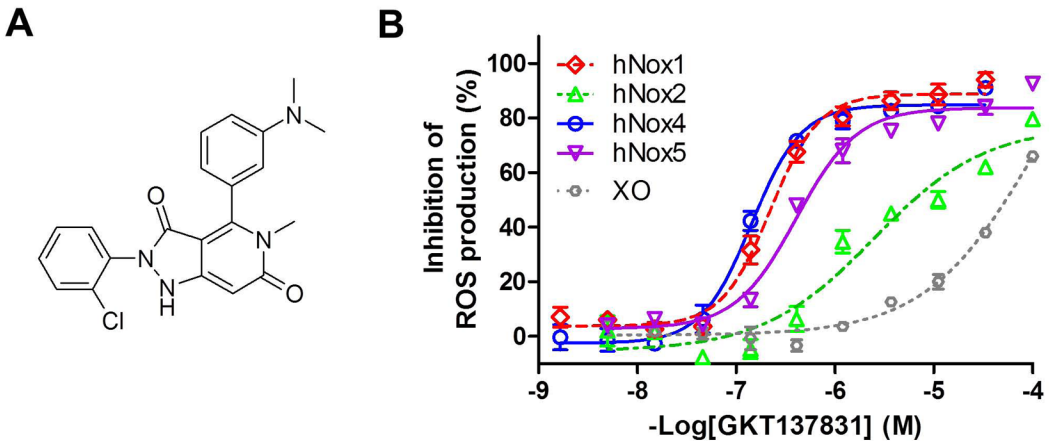

C

	Ki (nM)				
	Nox1	Nox2	Nox4	Nox5	XO
GKT137831	140±40	1750±700	110±30	410±100	> 100 μM
DPI	60	70	70	75	50

Fig. 2. Pharmacological profile of GKT137831, a dual Nox1/Nox4 inhibitor

(A) Chemical structure of the dual Nox1/Nox4 inhibitor GKT137831. (B) Inhibition of Nox-dependent ROS production by GKT137831: concentration-response curves of GKT137831 on membranes prepared from cells specifically overexpressing hNox1 (◇), hNox2 (△), hNox4 (○), hNox5 (▽) and on Xanthine Oxidase (XO) (○). Km of NADPH for hNox1, hNox2, hNox4 and hNox5 and was 70±10mM, 16±3mM, 120±20mM and 70 ±10mM respectively and Km of Xanthine for XO was 6±1mM. Results are from one experiment performed in triplicate, representative of at least three performed. Values are means±SEM. (C) Inhibition constants (Ki) of GKT137831 and DPI on hNox1, hNox2, hNox4, hNox5 and XO.

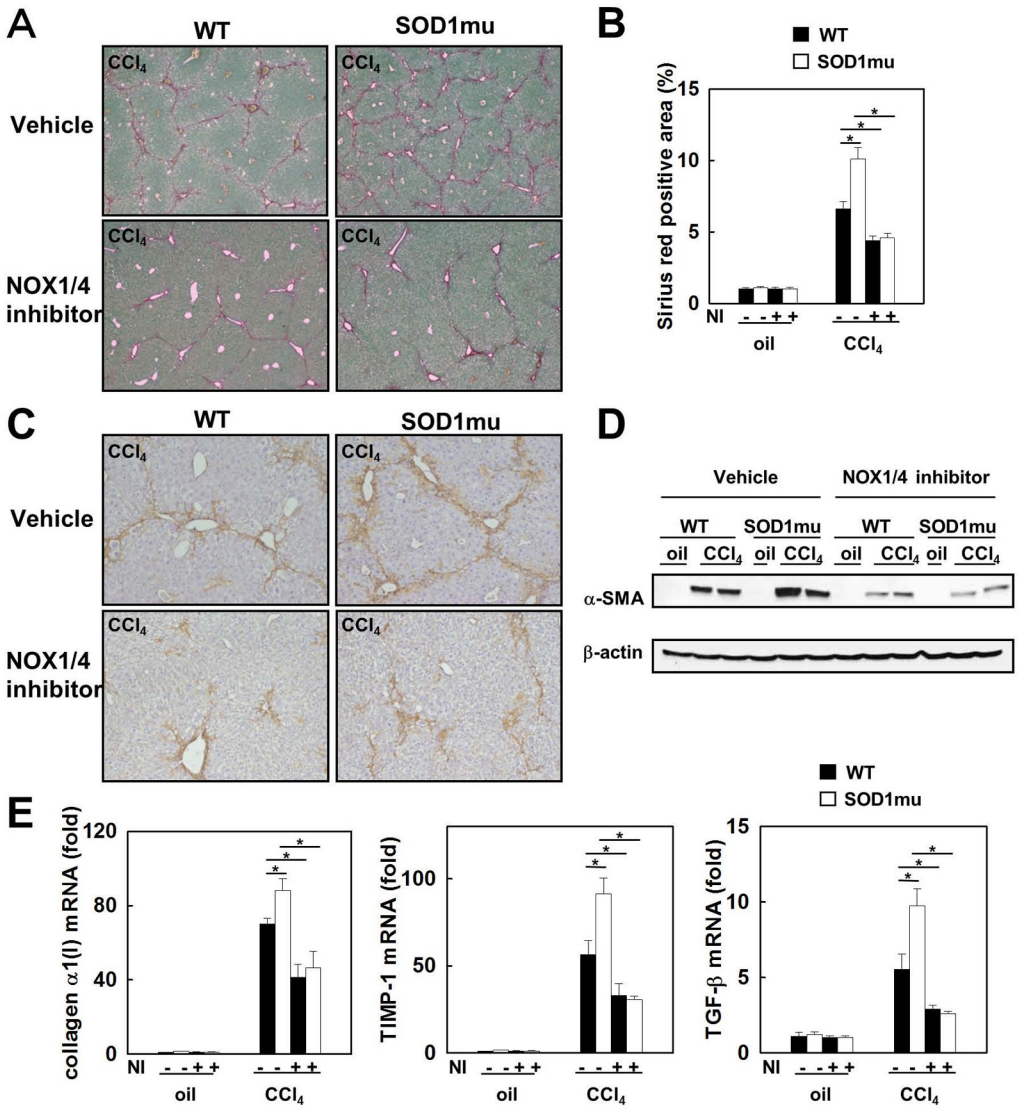

Fig. 3. Enhanced liver fibrosis in SOD1mu mice is suppressed by inhibition of NOX1/4 with GKT137831

Livers from WT or SOD1mu mice were analyzed after 12 injections of CCl_4 or vehicle (n=5). In last half period of injections, some mice in each strain were treated by NOX1/4 inhibitor daily. (A) Fibrillar collagen deposition was evaluated by sirius red staining (original magnification ×40), and (B) its quantification is shown. The expression of a-SMA in the liver was detected by (C) immunohistochemistry staining and (D) Western blotting (original magnification ×100). (E) Hepatic expression of collagen α1(I), TIMP-1 and TGF-β1 mRNA was measured by quantitative real-time PCR. NI: NOX1/4 inhibitor. *P<0.05

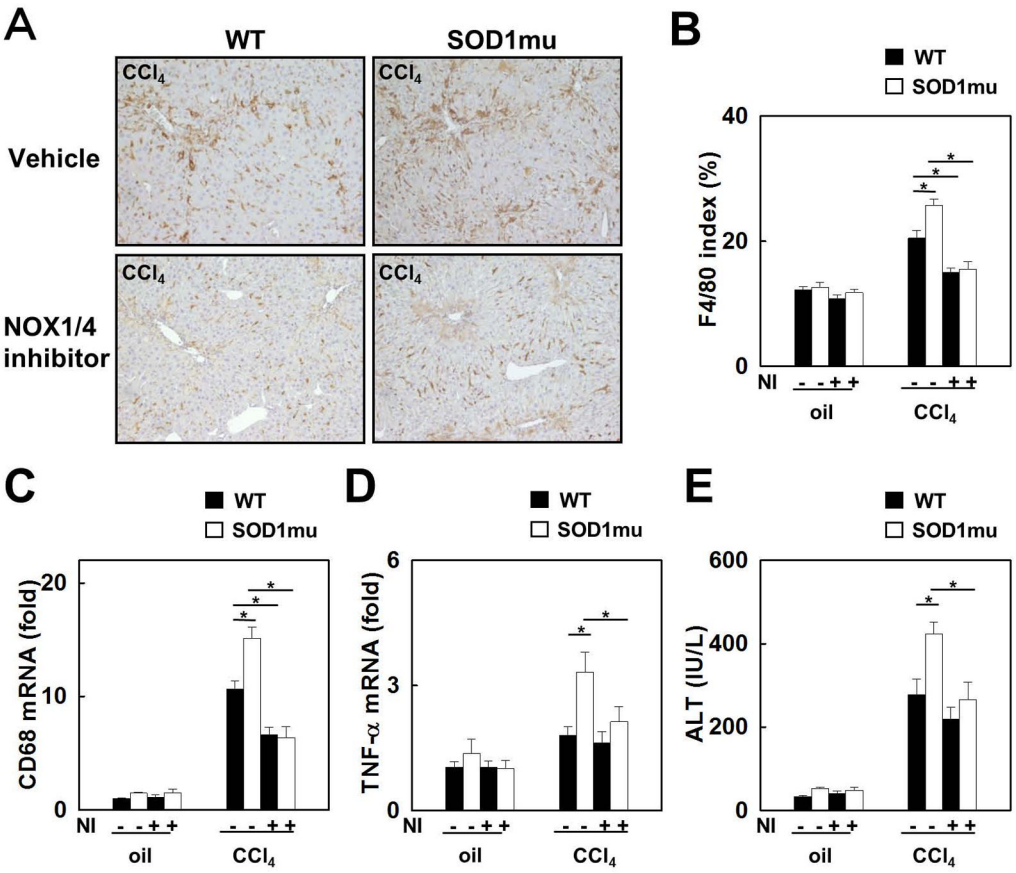

Fig. 4. Enhanced liver inflammation in SOD1mu mice is suppressed by NOX1/4 inhibition

Livers from WT or SOD1mu mice were analyzed after 12 injections of CCl_4 or vehicle (n=5). In last half period of injections, some mice in each strain were treated by NOX1/4 inhibitor daily. Immunohistochemistry for (A) F4/80 and (B) its quantification are shown (original magnification ×100). (C, D) Hepatic mRNA expression of CD68 and TNF-α was measured by quantitative real-time PCR. (E) Serum ALT levels were measured. NI: NOX1/4 inhibitor. *P<0.05

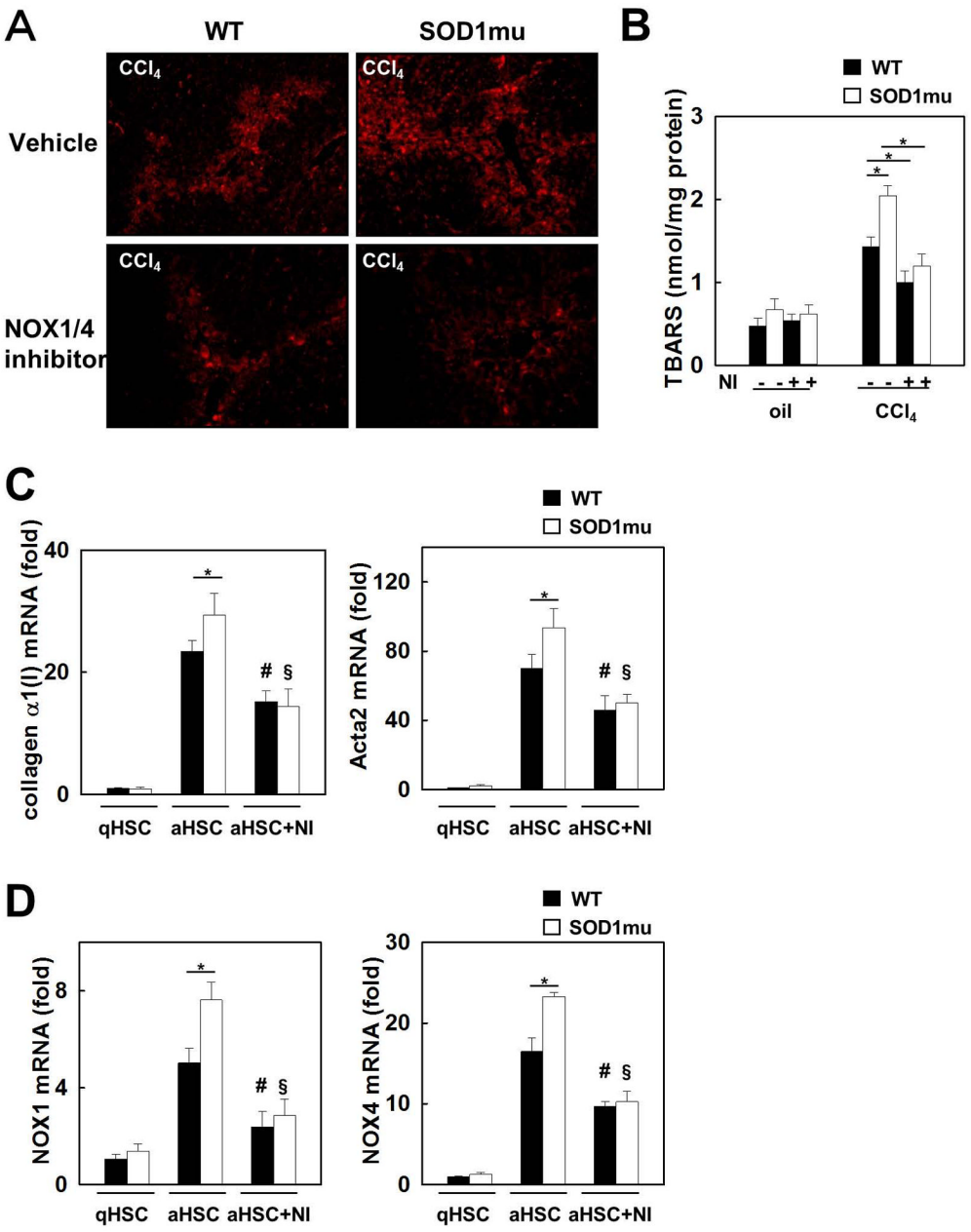

Fig. 5. Enhanced lipid peroxidation and expression of fibrogenic genes in SOD1mu mice was reduced by NOX1/4 inhibition

(A) Livers from WT or SOD1mu mice were analyzed after 12 injections of CCl_4 or vehicle (n=5). In last half period of injections, some mice in each strain were treated by NOX1/4 inhibitor daily. Representative images of 4-hydroxynonenal (4-HNE) immunofluorescent staining (original magnification ×100). (B) Hepatic malondialdehyde levels were measured in livers from (A) using thiobarbituric acid reactive substances (TBARS) assay. NI: NOX1/4 inhibitor. *P<0.05. HSCs isolated from WT or SOD1mu mice were incubated with NOX1/4 inhibitor (20 μM) or vehicle (n=3). mRNA levels of (C) collagen α1(I) and Acta2 and (D) NOX1 and NOX4 were measured by quantitative real-time PCR. qHSC: quiescent HSC. aHSC: activated HSC. NI: NOX1/4 inhibitor. *P<0.05. #P<0.05 compared to WT aHSC. §P<0.05 compared with SOD1mu aHSC.

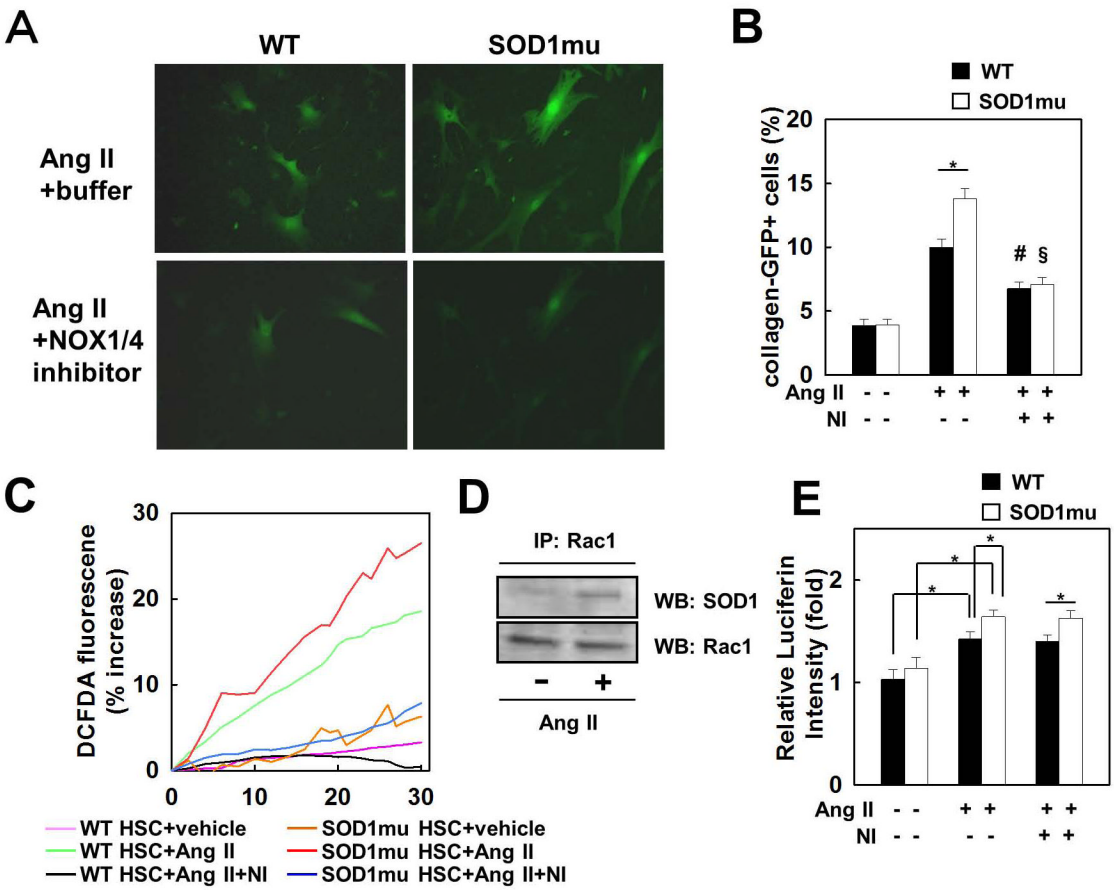

Fig. 6. Increased fibrogenic response and ROS production stimulated by Ang II in SOD1mu HSCs are suppressed by NOX1/4 inhibition

HSCs isolated from WT and SOD1mu colI-GFP transgenic mice were stimulated by Ang II (10^{-6} M), with NOX1/4 inhibitor (20 μM), or vehicle for 24 hours (n=3). (A) Representative photomicrographs of GFP-positive HSCs and (B) their quantification are shown (original magnification ×200). *P<0.05, #P<0.05 compared to WT HSC stimulated by Ang II. §P<0.05 compared to SOD1mu HSC stimulated by Ang II. (C) HSCs from WT and SOD1mu mice were loaded with redox-sensitive dye CM-H_2DCFDA (10 μM) for 20 minutes. Cells were then washed twice and subsequently stimulated by Ang II (10^{-6} M) with NOX1/4 inhibitor (20 μM) or vehicle. Fluorescence signals were quantified continuously for 30 minutes using fluorometer (n=3). (D) Rac1 immunoprecipitation (IP) from cell extracts from human HSC LX-2 cell line followed by Western blot (WB) for SOD1 or Rac1. (E) WT or SOD1mu HSCs were stimulated by Ang II with NOX1/4 inhibitor (20 μM) or vehicle for 24 hours. Rac1 activity was measured by ELISA (n=3). Ang II: angiotensin II, NI: NOX1/4 inhibitor. *P<0.05.

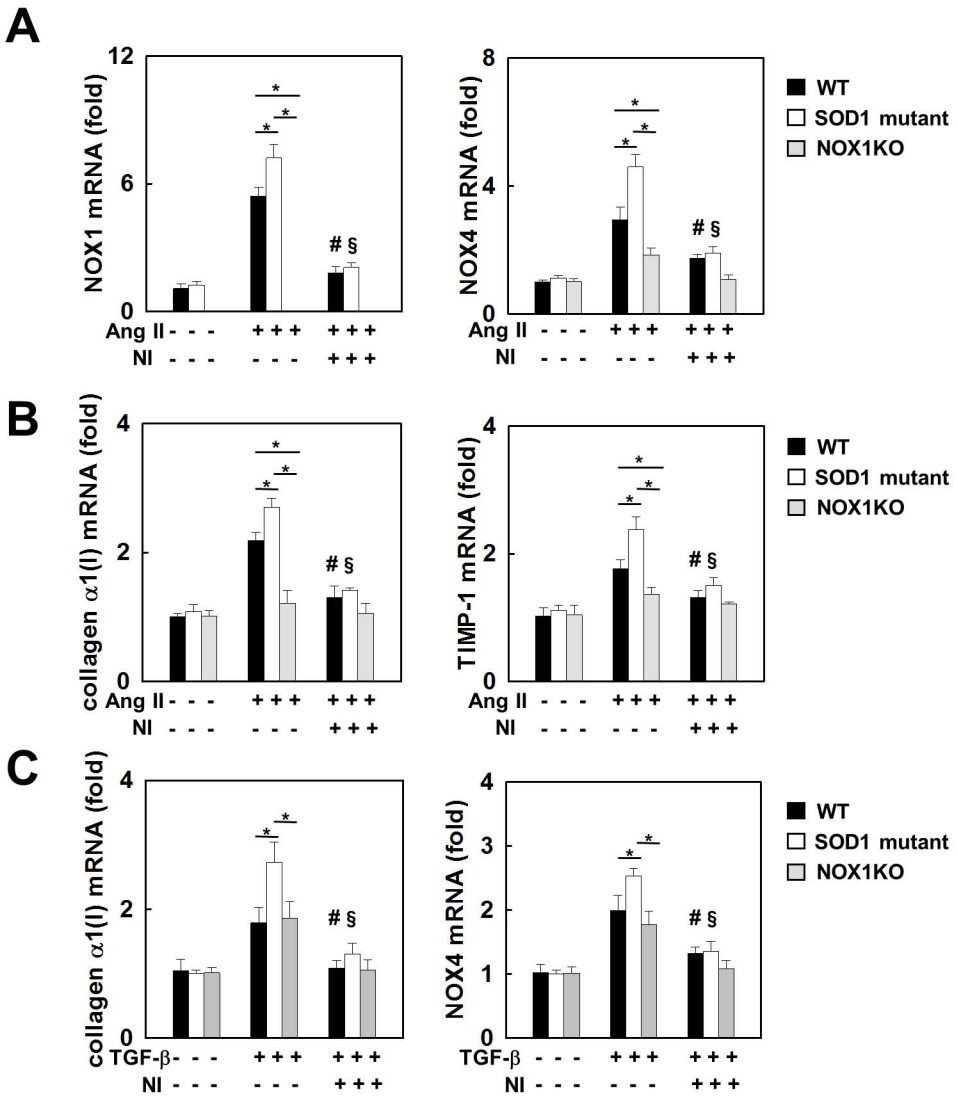

Fig. 7. Upregulation of NOX4 by Ang II and TGF-β

HSCs isolated from WT, SOD1mu, and NOX1KO mice were stimulated by Ang II (10^{-6} M), TGF-β (10 ng), with NOX1/4 inhibitor (20 μM), or vehicle for 24 hours (n=3). mRNA levels of (A) NOX1 and NOX4, and (B) collagenα1(I) and TIMP-1 in HSCs after Ang II stimulation. (C) mRNA levels of collagen α1(I) and NOX4 after TGF-β stimulation. Ang II: angiotensin II, NI: NOX1/4 inhibitor. *P<0.05. #P<0.05 compared to WT HSC stimulated by Ang II or TGF-β. §P<0.05 compared to SOD1mu HSC stimulated by Ang II.